Journal of Engineering and Applied Sciences 13 (24): 10297-10305, 2018
ISSN: 1816-949X
© Medwell Journals, 2018

Thermo-Hydraulics of Flow Through Helical and Straight Pipes

[1]Saba Yassoub Ahmed and [2]Zainab Hussain Alammar
[1]Department of Mechanical Engineering, College of Engineering, University of Babylon, Babylon, Iraq
[2]Department of Mechanical Engineering, College of Engineering, University of Al-Mustaqbal, Hillah, Iraq

Abstract: An experimental and numerical investigation has been conducted on pressure drop and steady-state natural convection heat transfer from vertical helical cultures in the heat transfer water bath. The helical coiled tube is formed by bending a straight copper tube has diameter 12.5 mm into a helical-coil of 4.5 turns. The helical coiled tube under constant water bath temperature at 70°C is tested, cold water worked as the target fluid is flow in helical coil from down to up direction at flow rate range 10-25 L/min. The turbulent flow and heat transfer developments are simulated by using the k-ε standard turbulences model. A finite volume methode with an unstructured non-uniform gride system is employed for solving the model. The comparison is also, made numerically between the heat exchange and pressure drop in helical coil pipe with that in a straight pipe. The results show that the good agreement between the numerical results and the experimental data. The centrifugal force has a significant effectt on the enhancements of heat transfer and pressure drop. In addition, due to this force, the heat transferrand pressure drop obtained from the helically coiled tube are higher than those of the straight tube.

Key words: Helical coil heat exchanger, natural convection heat transfer, pressure drop, turbulent flow, numerical results, non-uniform

INTRODUCTION

Today becomes need to increase the heat transfer performance of heat exchangers in order to reduce the energy and material consumption as well as the associated impact of environmental degradation has led to the development and usage of many heat transfer enhancement techniques. Enhancement can be achieved by increasing the convection heat transfer coefficient and the convection surface area. Different methods have been developed and they are characterized as either passive or active technique. In active technique the heat transfer rate is improved by supplying an extra energy to the system such as fluid vibration, electric field and surface vibration. While for passive technique generally, consist of geometric or material modification of the primary heat transfer and examples include finned surfaces, swirl flow that producing by inserting (turbolater) and coiled tubes, among others.

Coiled tube is one method of passive techniqueuse to enhance the heat transfer characteristic by producing the centrifugal force and this increase the flow turbulent. Any increase in heat transfer causes to increase the pressure drop due to increased frictional losses. Coiled tubes are used in heat exchangers, condensers and evaporators in food processing, chemical engineering, refrigeration, air conditioner and nuclear reactors due to several advantages of coils such as: a coil provide a large surface area in relatively small reactor volume and give a better heat transfer performance, since, they have a lower wall resistance and high process side coefficient. Fouling factor is less in helical coil type than that of shell and tube type due the turbulence created inside it. At the same time have different disadvantages such as: cleaning of vessel in more difficult than the shall and jackets with coils and highly corrosive fluid cannot be used.

An experimental and numerical study has been made by Janssen and Hoogendoorn (1978) on the convective heat transfer for coiling pipes. The experimental have been carried out for pipe to coil Diameter ratios (d/D) range (0.01-0.1), Prandtl number range (10-500) and Reynolds number range (20-4000), the heat transfer has been studied for both uniform peripherally averaged heat flux and constant wall temperature, the results showed that the heat transfer coefficient enhancement in coiled tube due to the effect of the centrifugal force. Kozo and Yoshiyuki (1988) studied numerically the effect of the secondary flow into three types: in the centrifugal, the buoyancy and the composite range. At low Reynolds numbers for the flow through coiled tube the centrifugal

Corresponding Author: Saba Yassoub Ahmed, Department of Mechanical Engineering, College of Engineering, University of Babylon, Babylon, Iraq

flow field due to the centrifugal force is weak. So, the coiled pitch (distance between two adjutens turns) has significant effected on the friction factor and Nusslet number (Austen and Soliman, 1988). Steady state turbulent natural convection heat transfer from vertical helical coiled tubes to water has been studied experimentally by Ali (1994). The data are correlated with the Rayleigh number for two different coil sets. The first set has d_o = 0.012 m and three D/d_o of (20.792, 13.923 and 9.941) And the second set has d_o = 0.008 m and two D/d_o of (19.957 and 9.941) with a number of turns 5 and 10, respectively. The results show for the first set that the heat transfer coefficient decreases with the increase number of turns while decreases for the second set. The natural convection heat transfer from helicoidal pipe with vertical and horizontal orientation have been studied experimentally by Xin and Ebadian (1996) for Rayleigh numbers range ($4*10^3$-$1*10^5$) for vertical coils and ($5*10^3$-$1*10^5$) for horizontal coils with curvature ratio (d/D) = 0.1 and the tube diameter change from (12.5-25.4 mm). The results showed that the Nusselt number on the outer side of the coil is higher than that on the inner side at the middle turns also; The Nusselt number of the horizontal coil is higher than that of the vertical coil in the laminar region. The last experimental have been completed and developed by Ali (1998) by using a horizontal helicalcoil pipe and subjected to a uniform heat flux from the air. The experimental data have been obtained for four coils with a range of heat flux 500-5000 W/m^2. The results have been shown that the heat transfer coefficient decrease as the number of turns increase. Prahhanjan (2000) designed and built a water bath thermal processor to study the influence of helical coil characteristic on heat transfer to Newtonian fluids such as water and base oil that have three different viscosities. Ali (2001) and Coronel and Sandeep (2003) shows the effected of the Reynolds number and curvature ratio on the pressure drop and friction factor. The correlation equations have been developed for both of them. Moawed (2005) presented in experimental study the effected of the different coil parameters such as: pitch to pipe diameter ratio (p/d), coil to pipe Diameter ratio (D/d) and Length to pipe diameter ratio (L/d) on the local Nusselt number and showed that the Nusselt number for the coiled tube in horizontally oriented is greater than vertical oriented by about 12%. Coronel and Sandeep (2008) studied experimentally the convection heat transfer coefficient in both helical and straight tubular heat exchangers under turbulent flow conditions. The results showed that the overall heat transfer coefficient (U) in the helical heat exchanger was much higher than that a straight tubular heat exchangers. In addition, the heat transfer coefficient has proportional directional with the curvature ratio (d/D). The other boundary condition were used by Shokouhmand *et al.* (2008) and Salimpour (2009) which investigated experimentally the heat transfer coefficients of shell and helically coiled tube heat exchangers alsot studied the effect of the coil pitch and the curvature ratio on the heat transfer coefficient. Ghorbani *et al.* (2010) studied experimentally the effective of the tube parameters on the performance coefficient. The forced convective heat transfer in straight and coiled tubes having smooth and corrugated wall was experimentally investigated by Rainieri *et al.* (2012) with tube diameter 14 mm, a curvature ratio 0.06, a corrugation depth 1 mm and a corrugation pitch 16 mm. The main conclusion was that the wall curvature enhanced the heat transfer at all the Reynolds number (Re) whereas the wall corrugation enhanced the heat transfer only in the higher Re range Mohammed (2011), Purandare *et al.* (2012) and Pawar and Sunnapwar (2013) showed that the heat transfer coefficient and Nusselt number increase as the diameter ratio increases. Pandey *et al.* (2014) showed in experimental and numerical study that the friction factor decreases as Dean number increases whereas pressure drop increases as the Reynolds number increases. Ciofalo *et al.* (2014) and Gunjo *et al.* (2015) studied numerically the pressure drop and the heat transfer in helically coiled pipe heat exchanger at turbulent regime.

The previous researches have been shown that the secondary flow as a resulting from the centrifugal force causes the heat transfer coefficient to be significantly higher. In the present research studied numerically and experimentally the pressure drop and outside Nusselt number for natural convection heat transfer from turbulent flow coiled pipe immersed in vertical oriented in hot bath water and then comparing the results with that similar a straight pipe setup which modeled by ANSYS-Fluent 14 Software and operating under a similar conditions since its very expensive if its research experimentally.

Literature review

Experimental setup: A schematic diagram of the experimental apparatus is sketched in Fig. 1. The testing coiled tube (1) is formed from straight pipe made from copper have an outer diameter (12.5 mm) and thickness (1 mm), filling the straight pipe with fine sand and then wound on a cylinder stand of the desired diameters to form the helical coil and this was pushed out with compressor to obtain the smoothness of the inner surface. The outer turn Diameter (Ds) is measured for each turn and then the helix coil diameter can be calculated from the Eq. 1, the coil length is calculated from $L = \pi D_s N$ (Ali, 1994). The physical dimensions shown in Fig. 2:

$$D_s = \frac{\sum_{i=1}^{n}\sqrt{\left(D_i^2 - \left(\frac{P}{\pi}\right)^2\right)}}{N} \quad (1)$$

The coil is oriented vertically in the insulated rectangular tank Eq. 2, this tank working as a heating medium has dimensions 60*60*120 cm and filled with water and heated by three 9 h each one with 6000 W that located in the bottom two were at all time and the last one was used as wanted to keeping a constant water bath at 70°C. The flow of the cold water is pumped through the coil by two centrifugal pumps Eq. 3 to maintain the

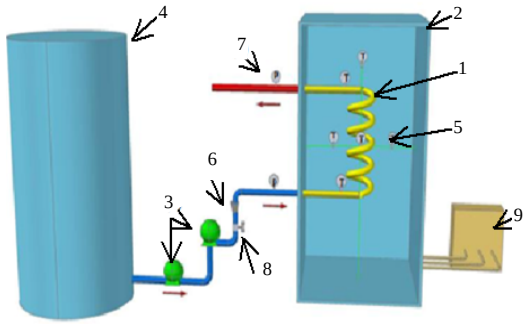

Fig. 1: Schematic diagram of the experimental apparatus: 1) Test section (helical pipe); 2) Rectangular tank; 3) Two series centrifugal pump; 4) Reservoir tank; 5) Thermocouple; 6) The volumetric flow meter; 7) Pressure tap; 8) Valve and 9) Electric heaters

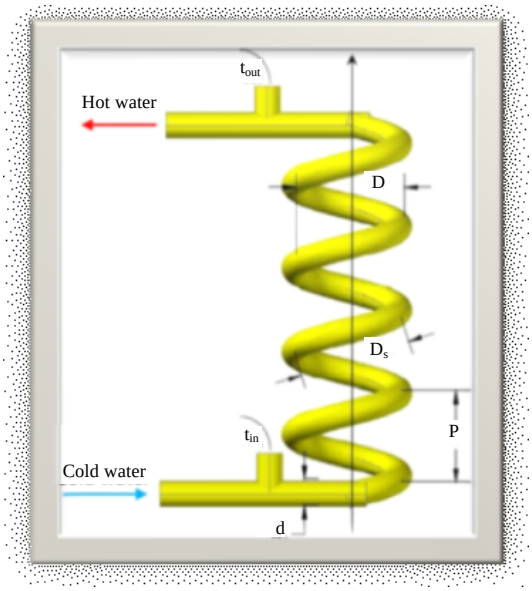

Fig. 2: Schematic of the coil used to show the physical dimensions and thermocouples location

volume flow rate range 10-25 L/min. The volume flow rate through the coil is measured by a flow 6 m (type FLOTECH of range 10-70 L/min). Two thermocouple (5) (K-type, pin wire, range: 0-800°C) used to measure the water temperature at inlet, outlet of the helical coil, its located shown in Fig. 2 and four used to measure the water bath temperature. Digital pressure 7 nm (type Lurton PM-9107, ±7000 mbar (7 bar) maximum range) was used to measure the pressure difference between the coil ends.

MATERIALS AND METHODS

Uncertainty: In this research, the estimation of the experimental uncertainty is based on the approach presented by Holman and Gajda (1989), Anonymous (2006). The individual experimental uncertainty of the measured variables with the calculated are given in Table 1. The analysis is dependent on the maximum percentage error in the parameters.

Experimental calculations: The total amount of heat transferred from the water bath to the coiling pipe was calculated as shown as:

$$Q = m.cp.(T_{out} - T_{in}) \quad (2)$$

The overall heat transfer coefficient could be calculated from:

$$U_o = q/(A_o \cdot \Delta T) \quad (3)$$

Where:

$$\Delta T = \left(T_{bath} + (T_{in} + T_{out})/2\right)/2$$

$$U_o = 1/\left((1/h_o) + (r_o \ln(r_o/r_i)/k) + (r_o * h_i/r_i)\right) \quad (4)$$

In the Eq. 4, the inside heat transferr coefficient cambia determine from the inside Nusselt number

Table 1: Uncertainty of measured variables and calculated parameters

Independent variables	Uncertainties (%)
Pressure drop (Δp)	2.00
Flow rate (m)	2.50
Length (L)	0.05
Density (ρ)	0.10
Specific heat (cp)	0.10
Viscosity (μ)	0.10
Thermal conductivity (K)	0.01
Coil Diameter (D)	0.01
Tube diameter (d)	0.01
Average bulk temperature (ΔT_b)	0.706
Average film temperature (ΔT_F)	0.706
Heat transfer coefficient (h_o)	$2.4167*10^2$
Nusselt number (Nu_o)	$4.3567*10^3$

Table 2: Physical dimensions

Variables	d (mm)	N	P (mm)	D (mm)	L (m)	T_{bath} (°C)	$\dot{m}$ (L/min)
Helical coil	12.5	4.5	12.5	200	2.827	70	10-25
Straight pipe	12.5	-	-	-	-	2.827	70

Rectangular tank; Dimensions = 60*60*120 (cm); Cylindrical tank; Cylindrical diamete r = 100 (pipe diameter)

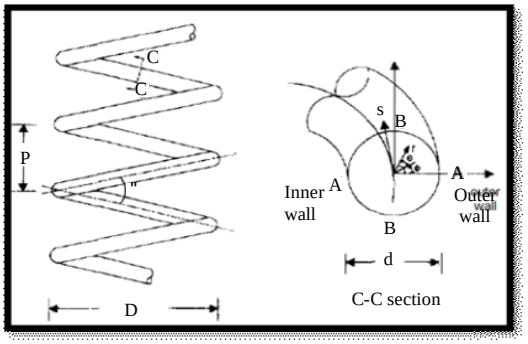

Fig. 3: The coordinate system

which based on the equation below (Rogers and Mayhew, 1964; Prabhanjan *et al*., 2004; Ali, 2006):

$$Nu_i = 0.021Re^{0.85}Pr^{0.4}\left(r_i/R\right)^{0.1} \quad (5)$$

The inside heat transfer coefficient, h_i was then calculated:

$$h_i = Nu_i.K/2.r_i \quad (6)$$

The new wall temperature, T_w was then calculated from

$$T_w = \left(q/\left(h_i.A_i\right)+T_{bath}\right. \quad (7)$$

An iteration procedure was repeated until a convergence was received by Fortran 90 computer program. The outside heat transfer coefficient was then calculated from the thermal resistance equation.

Mathematical modeling: The geometry system in the present work is divided into two models: first model for coiling pipe in a large water bath in order to house the coiling pipe while the second model of a straight pipe in a large cylindrical water bath. The two models are modeled in a 3D structure with all dimensions as mention in the Table 2 by using the design modeling in the ANSYS Workbench 14.0.

The helicoidal pipe has the coordinates as shown in Fig. 3. S-axial dimensional coordinate, r-Radial dimensional coordinate and Ψ = 0+Φ-tangential coordinate. Before giving any details for the governing equations, it must be given the assumptions to simplify the problem which are: the flow is assumed to be steady incompressible, three dimensional, Newtonian, single phase and turbulent flow. All the properties of the flow are assumed to be a polynomial function of temperature. The governing equations can be written as (Yang and Ebadian, 1996; Beckwith *et al*., 2007).

Continuity equation:

$$\frac{1}{r}\frac{\partial u}{\partial \Psi}+\frac{\partial v}{\partial r}+\frac{v}{r}+\delta\omega\left(u\cos\Psi+v\sin\Psi-\lambda\frac{\partial w}{\partial \Psi}\right)=0 \quad (8)$$

Momentum equation:

$$\begin{aligned}&\Psi\text{- coordinate }\rho\left(\frac{\partial(uu)}{r\partial\Psi}+\frac{1}{r}\frac{\partial(ruv)}{\partial r}\right)=-\frac{1}{r}\frac{\partial p}{\partial\Psi}+\\&\rho\delta_w\omega\left(w\cos\Psi+\lambda\frac{\partial u}{\partial\Psi}\right)-\rho\frac{uv}{z}-\rho u\delta\omega\left(u\cos\Psi+v\sin\Psi-\lambda\frac{\partial w}{\partial\Psi}\right)+\\&\frac{1}{r}\frac{\partial}{\partial r}\left(r\tau_{r\Psi}\right)+\frac{\partial}{r\partial\theta}\left(\tau_{\Psi\Psi}\right)+\frac{\tau_{r\Psi}}{r}+\\&\delta\omega\left(\tau_{\Psi\Psi}\cos\Psi+\tau_{r\Psi}\sin\Psi+\tau_{ss}\cos\Psi\right)-\delta\omega\lambda\frac{\partial}{\partial\Psi}\tau_{\Psi S}\end{aligned} \quad (9)$$

r-coordinate:

$$\begin{aligned}&\rho\left(\frac{1}{r}\frac{\partial(uv)}{\partial\Psi}+\frac{1}{r}\frac{\partial(rvv)}{\partial r}\right)=-\frac{\partial p}{\partial r}+\\&\frac{1}{r}\frac{\partial(r\tau_{rr})}{\partial r}+\frac{1}{r}\frac{\partial\tau_{r\Psi}}{\partial_\Psi}+\rho\delta\omega w\times\left(w\sin\Psi+\lambda\frac{\partial v}{\partial\Psi}\right)+\rho\frac{u^2}{r}-\\&\rho v\delta\omega\times\left(u\cos\Psi+v\sin\Psi-\lambda\frac{\partial w}{\partial\Psi}\right)-\frac{\tau_{\Psi\Psi}}{r}+\delta\omega\times\\&\left(\tau_{r\Psi}\cos\Psi+\tau_{rr}\sin\Psi-\tau_{ss}\sin\Psi\right)-\delta\omega\lambda\frac{\partial}{\partial\Psi}\tau_{rs}\end{aligned} \quad (10)$$

s-coordinate:

$$\begin{aligned}&\rho\left(\frac{\partial(uw)}{r\partial\Psi}+\frac{1}{r}\frac{\partial(rvw)}{\partial r}\right)=-\omega\frac{\partial p}{\partial s}+\\&2\rho w\omega\delta\left(u\cos\Psi+v\sin\Psi-\lambda\frac{\partial w}{\partial\Psi}\right)\tau_{\Psi s}+\frac{1}{r}\frac{\partial}{\partial r}\left(r\tau_{rs}\right)+\\&2\delta\omega w\left(\tau_{\Psi s}\cos\Psi+\tau_{rs}\sin\Psi\right)\end{aligned} \quad (11)$$

Energy equation:

$$\begin{aligned}&\rho\left(\frac{1}{r}\frac{\partial(uT)}{\partial\Psi}+\frac{1}{r}\frac{\partial(rvT)}{\partial r}\right)=\Gamma_T\left(\frac{1}{r^2}\frac{\partial^2T}{\partial\Psi^2}+\frac{\partial^2T}{\partial r^2}+\frac{1}{r}\frac{\partial T}{\partial r}\right)-\\&\rho\omega w\frac{\partial T}{\partial s}-\rho T\left[\delta\omega\left(u\cos\Psi+v\sin\Psi-\lambda\frac{\partial w}{\partial x}\right)\right]+\rho w\omega\delta\lambda\frac{\partial T}{\partial\Psi}+\\&\Gamma_T\left[\omega\delta\left(\frac{1}{r}\frac{\partial T}{\partial\Psi}\cos\Psi+\frac{\partial T}{\partial r}\sin\Psi\right)+\rho\lambda^2\delta^2\omega^2\left(\frac{\partial^2T}{\partial\Psi^2}+\omega\delta r\cos\Psi\frac{\partial T}{\partial\Psi}\right)\right]\end{aligned} \quad (12)$$

Turbulent Model (k-ε Model); Kinetic energy equation:

$$\rho\left[\frac{1}{r}\frac{\partial(uk)}{\partial\Psi}+\frac{1}{r}\frac{(rvk)}{\partial r}\right]=\frac{\Gamma_k}{\sigma_k}\left[\frac{1}{r^2}\frac{\partial^2 k}{\partial\Psi^2}+\frac{\partial^2 k}{\partial r^2}+\frac{1}{r}\frac{\partial k}{\partial r}\right]-\rho k\left[\delta\omega\left(u\cos\Psi+v\sin\Psi-\lambda\frac{\partial w}{\partial\Psi}\right)\right]+\rho w\omega\delta\lambda\frac{\partial k}{\partial\Psi}+$$
$$\frac{\mu_t}{\sigma_k}\left[\omega\delta\left(\frac{1}{r}\frac{\partial k}{\partial\Psi}\cos\Psi+\frac{\partial k}{\partial r}\sin\Psi\right)+\rho\lambda^2\delta^2\omega^2\left(\frac{\partial^2 k}{\partial\Psi^2}+\omega\delta r\cos\Psi\frac{\partial k}{\partial\Psi}\right)\right]+G-\rho\varepsilon \quad (13)$$

Kinetic energy dissipation equation:

$$\rho\left(\frac{1}{r}\frac{\partial(u\varepsilon)}{\partial\Psi}+\frac{1}{r}\frac{(rv\varepsilon)}{\partial r}\right)=\frac{\Gamma_\varepsilon}{\sigma_\varepsilon}\left[\frac{1}{r^2}\frac{\partial^2\varepsilon}{\partial\Psi^2}+\frac{1}{r}\frac{\partial\varepsilon}{\partial r}\right]-\rho\varepsilon\left[\delta\omega(u\cos\Psi+v\sin\Psi-\lambda\frac{\partial w}{\partial\Psi}\right]+\rho w\omega\delta\lambda\frac{\partial\varepsilon}{\partial\Psi}+$$
$$\frac{\mu_t}{\sigma_\varepsilon}\left[\omega\delta\left(\frac{1}{r}\frac{\partial e}{\partial\Psi}\cos\Psi+\frac{\partial\omega}{\partial r}\sin\Psi\right)+\rho\lambda^2\delta^2\omega^2\left(\frac{\partial^2\omega}{\partial\Psi^2}+\omega\delta r\cos\Psi\frac{\partial\omega}{\partial\Psi}\right]+c_1\frac{\omega}{k}G-\rho c_2\frac{\varepsilon^2}{k}\right. \quad (14)$$

The turbulent viscosity μ_t is defined ($\mu_t = c_\mu\rho k^2/\varepsilon$). The constants were used in this thesis for k and ε equations as follows (Beckwith *et al*., 2007; Launder and Spalding, 1972):

$$C_\mu = 0.09,\ C_{\varepsilon 1} = 1.47,\ C_{\varepsilon 2} = 1.92,\ \sigma_\tau = 0.07,\ \sigma_k = 1,\ \sigma_\varepsilon = 1.3$$

The generation term can be calculated by:

$$G=\mu_t\left\{2\left[\left(\frac{1}{r}\frac{\partial u}{\partial\theta}\right)^2+\left(\frac{v}{r}\right)^2+\left(\frac{\partial v}{\partial r}\right)^2+2\frac{v}{r^2}\frac{\partial u}{\partial\theta}+\omega^2\left[\delta\omega\left(u\cos\Psi+v\sin\Psi-\lambda\frac{\partial w}{\partial\Psi}\right)\right]^2-\frac{u}{r}\left(\frac{\partial v}{r\partial\theta}+\frac{\partial u}{\partial r}\right)-\omega\delta\lambda\left(\frac{1}{r}\frac{\partial u}{\partial\theta}\frac{\partial w}{\partial\theta}+\frac{\partial v}{\partial\theta}\frac{\partial\omega}{\partial r}\right)\right]+\left(\frac{\partial v}{r\partial\theta}+\frac{\partial u}{\partial r}\right)^2+\right.$$
$$\left.\left(\frac{u}{r}\right)^2+\left(\omega\delta\lambda\frac{\partial u}{\partial\theta}\right)^2+\left(\frac{1}{r}\frac{\partial w}{\partial\theta}\right)^2+(\omega\delta w)^2+\left(\frac{\partial w}{\partial r}\right)^2+\left(\omega\lambda\delta\frac{\partial w}{\partial\theta}\right)^2-2\omega\delta w\left[\cos\theta\left(\frac{1}{r}\frac{\partial w}{\partial\theta}-\omega\lambda\delta\frac{\partial u}{\partial\theta}\right)+\sin\theta\left(\frac{\partial w}{\partial r}-\omega\lambda\delta\frac{\partial v}{\partial\theta}\right)\right]\right\} \quad (15)$$

The mass flow rate is used as the inlet boundary condition and taken from experimental data with values 0.1667, 0.25, 0.333 and 0.416 kg/sec. the pressure also has been set as the inlet boundary and then corrected according to the outlet pressure that taken from experimental data while for energy equation has been used the inlet temperature of the flow as taken from experimental for each mass flow rate. The outlet boundary conditions for momentum equation are kept at a different value of pressure. The same procedure used for outlet temperature of the energy equation.

The commercial CFD codes estimate k and ε are based on turbulence intensity, i which is defined as the ratio of the root mean square of the velocity fluctuations U' to the mean flow velocity typically have values between 1-6%:

$$I=\frac{U'}{U_{avg}}=0.16\left(Re\ D_h\right)^{-1/8} \quad (16)$$

where, the D_h is the hydraulic diameter and equal to the diameter of the pipe. In the present study the turbulence Intensity (I) has been set to 5%. The wall boundary conditions for tank all the walls are adiabatic and the water bath remains constant at a temperature 70°C.

While for the coil are solved automatically with each iterative solution and the wall function method it must be used in order to find the boundary conditions at the solid wall. In the momentum equation the boundary conditions of the radial velocity is the no-slip while for both velocities in tangential and axial:

$$\mu_t=\left[\frac{y\left(c_\mu^{1.4}k^{1.2}\right)}{v}\right]\frac{\mu}{\ln(Ey+)/k}=\left\{\begin{matrix}\frac{y^+\mu}{u^+}\text{u velocity}\\ \frac{y^+\mu}{w^+}\text{w velocity}\end{matrix}\right\}= \quad (17)$$
$$\left\{\begin{matrix}\mu & y^+\le 11.5\\ \frac{\mu y^+}{2.51u\left(qy^+\right)} & y^+>11.5\end{matrix}\right\}$$

While the boundary conditions for the energy equation near the wall can be written as follows (Yang and Ebadian, 1996; Beckwith *et al*., 2007):

$$\Gamma_t=\left\{\begin{matrix}\frac{\mu}{pr_t}y^+\le 11.5\\ \frac{\mu y^+}{pr_t\left[2.51u\left(qy^+\right)+Be\right]}y^+>11.5\end{matrix}\right\} \quad (18)$$

$$B_e = 9\left(\frac{pr}{pr_t}-1\right)\left(\frac{pr}{pr_t}\right)^{\left(\frac{1}{4}\right)}\left.\frac{dk}{dr}\right|_{r=\text{surface tube}} = 0 \qquad (19)$$

Which it can be used in the kinetic energy equation the boundary condition for the dissipation rate ε near the wall:

$$\left(\epsilon_P = \frac{c_\mu^{3.4} k_P^{3/2}}{k\Delta y}\right)$$

where (P) denotes the next point to the solid wall.

Numerical computation: The numerical computations were carriedout by solving the governing conservations alongwith the boundary conditions using the finite volume method. The flow fieldwas solved using the simple algorithm. The second-order upwind differencing scheme is considered for the convective terms. The diffusion termin the momentum and energy equations is approximated by the second-order central difference which gives a stable solution. The effect of gravity force is applied in this analysis. The percentage imbalance of certain quantity is:

$$\frac{\left|\varnothing_{ij}^{n+1}-\varnothing_{ij}^{n}\right|}{\left|\varnothing_{ij}^{n+1}\right|} \le 10^{-4} \qquad (20)$$

Which is applied for all above equations momentum, energy and turbulent k-ε where the subscript i, j defined for each node and the superscript n represents the n-the iteration after convergence have been obtained for all equations then it can be calculated the Reynold number, Dean number and Nusselt number and finally the bulk temperature. Any CFD Software can be used a different type of mesh that comprising either structured or unstructured meshing. Structured meshes are used for a simple shaped while; Unstructured meshes that are useful for complex geometries Fluent User's guide, (Beckwith *et al*., 2007; Mohammed and Narrein, 2012).

In the current study used structured hexahedral mesh for the second model. While for the first model used unstructured mixed (hexahedral and tetrahedral) cells with a maximum and minimum size equal to 0.002 m through a high smoothing mesh near the wall of coiling and straight to give Y^+ <5 to solve the laminar sub layers as shown in Fig. 4.

To perform the grid independences by observing the convergent of the predicted mass flow rates with a given pressure drop at a various levels of grid refinement as

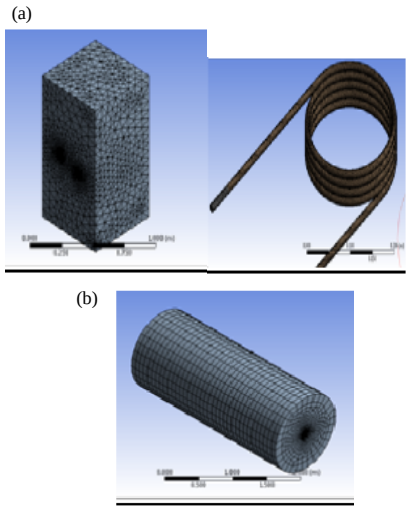

Fig. 4: Mesh type; a) Helical coil pipe and b) Straight pipe

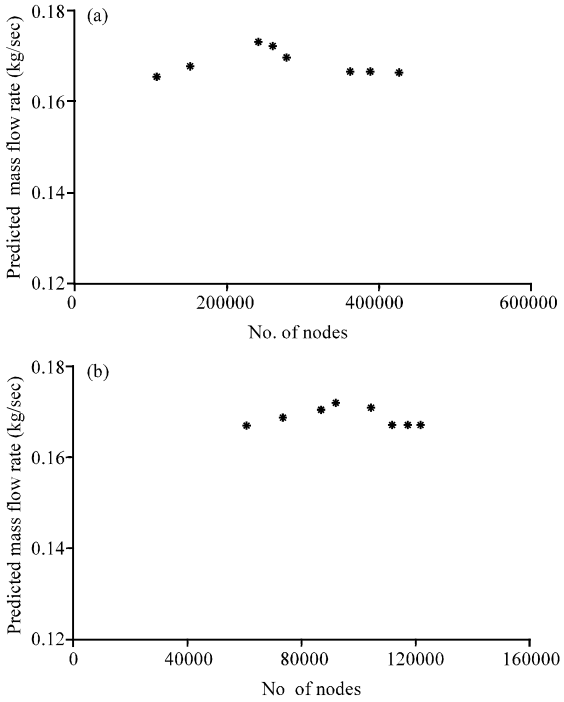

Fig. 5: Accuracy of mass flow rate prediction with number of nodes for; a) Helical coil and b) Straight pipe

shown in Fig. 5. It can be shown that the difference in mass flow rate was <0.5% as the nodes more than 25000 are employed for coiling pipe while for straight pipe more than 100000. Two adaptions have been used the first one depended on the pressure gradient that set to 0.1 and the second one depended on the Y^+ and set to 3 for the reason mentioned in the previous section.

RESULTS AND DISCUSSION

The numerical and experimental studies for heat transfer and pressure drop were conducted on the helical coiled and straight pipe heat exchanger. It can be shown in Fig. 6 that the temperature difference profile of the target fluid for both experimental and numerical reduced as the mass flow rate increased, depending on the residence time of fluid inside the coiling heat exchanger.

Figure 6 also, compares the results obtained from the present experiment and those from the numerical study. The maximum relative error between theoretical and numerical was 1.15615%.

Figure 7 shows the verification for Nusselt number with the volume flow rate. An increase in flow rate from 10 -25 L/min resulted in an increase in the Nusselt number due to the increase in heat transfer coefficient of the pipe. Considering the results obtained from the numerical study and those from the measured data, the maximum relative error produce was equal to 1.194%.

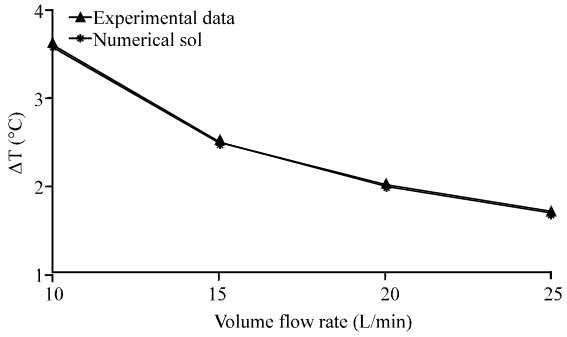

Fig. 6: Comparison of experimental and numerical temperature difference profile of the target fluid with the volume flow rate

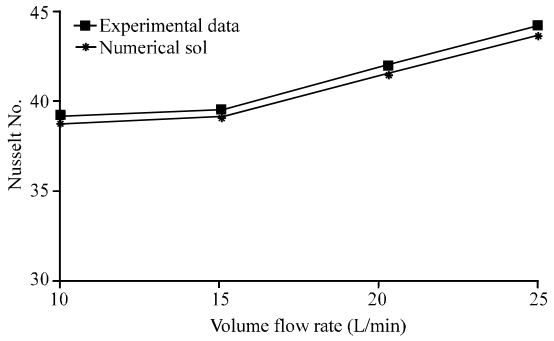

Fig. 7: Comparison of experimental and numerical outlet Nusselt number with the volume flow rate

The pressure drop is obtained from the experimental data and numerical model plotted against volume flow rate as in Fig. 8. Which shows that the pressure drop increased as the flow rate increase due to the effect of curvature ratio. These figures also show the comparison between the predicted results and the measured data the maximum relative error was 3.1%.

It can be shown that the development of the velocity magnitude (summation of the component velocity) along the axial dimensional distance (s) at different angles for the first turn, the fluid with uniform velocity occupies most of the cross section area (i.e., potential core). As the angle increases along the axial distance, the displacement effect of the growing boundary layer accelerates the flow in the main core, the unbalanced centrifugal force of the main flow results in the shift of the point of maximum velocity to the outside of the helical pipe, forming steeper gradient of the axial velocity near the outer wall.

While the development of the temperature field and the velocity magnitude contours for the third turn and angle 10° at the volume flow rate range 10-25 L/min. It can be shown that the temperature field is symmetric to the centerline connecting the outermost and the innermost points of the cross section as in the velocity contour.

When the axial distance is small, a fluid of uniform temperature occupies the most of the cross section area. While as the axial distance increases reach to the third turn, the shift of the velocity magnitude results in a shift of the temperature to the outside of the pipe, forming a steeper temperature gradient near the outer wall. Also, the increase of the volume flow rate results in an increase in the developing speed of the thermal boundary layer along the wall of the pipe.

As fluid flows within helical tube, it experiences a centrifugalis generated. A secondary flow induced by the

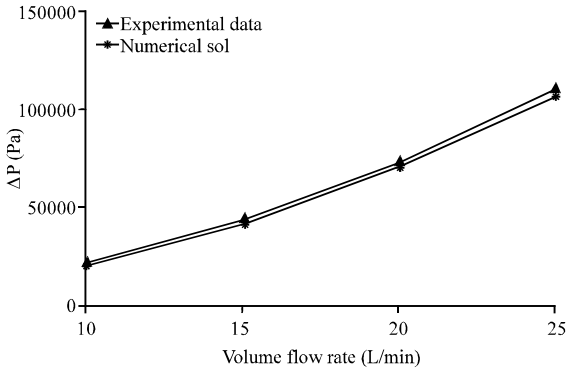

Fig. 8: Comparison of experimental and numerical of pressure drop of the target fluid with the volume flow rate

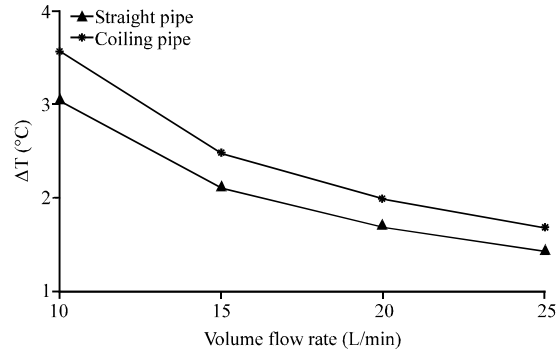

Fig. 9: The temperature difference for the straight and coiling pipe at a different flow rate

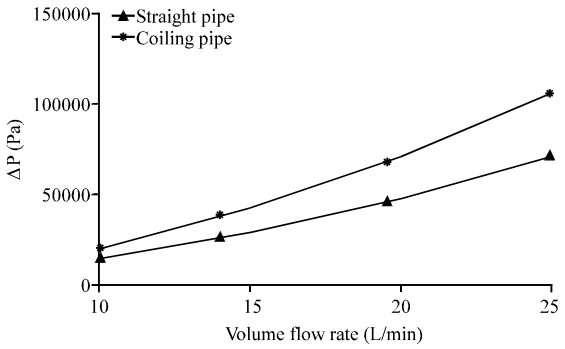

Fig. 11: Comparison the pressure drop of straight and coiling pipe for different flow rate

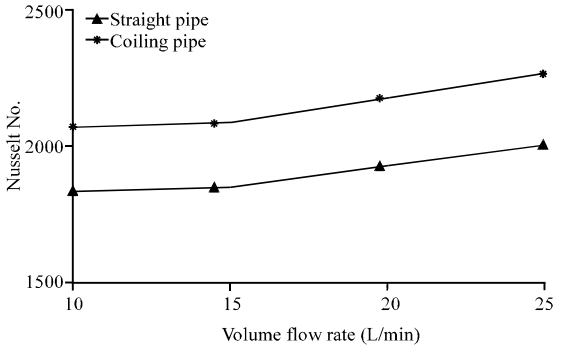

Fig. 10: Comparison outside Nusselt number of straight and coiling pipe for different flow rate

centrifugal force has significant ability to enhance the heat transfer rate by increasing the velocity gradient across the section of the tube and reduce the thermal boundary layer that formation on the tube wall surface. As a result, heat is transferred more rapidly in the helical tube. While when the fluid flow through the straight pipe, the fluid velocity is maximum at the tube center and then reduce near the pipe wall, this increase thickness of the thermal boundary layer, so that, the heat is conducted from the wall to the center it requires a substantial time to affect the fluid at the center.

So, the rise in temperature for the target fluid in coiling pipe being greater than the straight pipe by 17.64% as shown in Fig. 9. The Nusselt number has the same trend for characteristic length is the length of pipe as shown in Fig. 10 with an increase by 18.82% for coiling than that for straight pipe.

Figure 11 shows the pressure drop for both coiling and straight pipes. It can be shown that the pressure drop for coiling pipe was greater than that for straight pipe by 45.5%. The pressure drop in curved tube is related to a number of factors such as the friction between the fluid and the pipe wall and the pressure loss due to the change in elevation of the fluid (if the pipe not horizontal). Also, the presence of the secondary flow in curved pipe dissipates kinetic energy, thus, increasing the resistance to flow bends in pipes produced a greater head loss than if the pipe were straight.

CONCLUSION

The conclusion resulted from pervious numerical and experimental data was: the temperature difference of the target fluid for both experimental and numerical reduced as the mass flow rate increase while the outside Nusselt number has a proportional direction with the mass flow rate of the target fluid. The pressure drop for the flow through helical coil increase as the flow rate increase due to the effect of curvature ratio.

The centrifugal force increase as increase the axial distance, so, its cause a shift of the flow toward the outside of the pipeforming a steeper temperature gradient near the outer wall. Also, the increase of the volume flow rate results in an increase in the developing speed of the thermal boundary layer along the wall of the pipe. There are good agreements between the numerical and experimental data for both the heat transfer and pressure drop. Where the maximum relative error between theoretical and numerical was 1.15615% of the temperature difference, 1.194% for Nusselt number and 3.1% of the pressure drop.

The performance of the coiled pipe is better than for the straight pipe where the rise in temperature for the target fluid, Nusselt number and the pressure drop in coiling pipe are greater than in straight pipe by 17.64, 18.82 and 45.5%, respectively.

REFERENCES

Ali, M.E., 1994. Experimental investigation of natural convection from vertical helical coiled tubes. Intl. J. Heat Mass Transfer, 37: 665-671.

Ali, M.E., 1998. Laminar natural convection from constant heat flux helical coiled tubes. Intl. J. Heat Mass Transfer, 41: 2175-2182.

Ali, M.E., 2006. Natural convection heat transfer from vertical helical coils in oil. Heat Transfer Eng., 27: 79-85.

Ali, S., 2001. Pressure drop correlations for flow through regular helical coil tubes. Fluid Dyn. Res., 28: 295-310.

Anonymous, 2006. Fluent user's guide. Fluent, USA.

Austen, D.S. and H.M. Soliman, 1988. Laminar flow and heat transfer in helically coiled tubes with substantial pitch. Exp. Therm. Fluid Sci., 1: 183-194.

Beckwith, T.G., R.D. Marangoni and J.H.V. Lienhard, 2007. Mechanical Measurements. 6th Edn., Pearson, London, England, UK., ISBN:978-81-317-1718-9, Pages: 785.

Ciofalo, M., M. Di Liberto and G. Marotta, 2014. On the influence of curvature and torsion on turbulence in helically coiled pipes. J. Phys. Conf. Ser., 501: 1-13.

Coronel, P. and K.P. Sandeep, 2003. Pressure drop and friction factor in helical heat exchangers under nonisothermal and turbulent flow conditions. J. Food Process Eng., 26: 285-302.

Coronel, P. and K.P. Sandeep, 2008. Heat transfer coefficient in helical heat exchangers under turbulent flow conditions. Intl. J. Food Eng., 4: 1-12.

Ghorbani, N., H. Taherian, M. Gorji and H. Mirgolbabaei, 2010. An experimental study of thermal performance of shell-and-coil heat exchangers. Intl. Commun. Heat Mass Transfer, 37: 775-781.

Gunjo, D.G., P.K. Mahanta and P.S. Robi, 2015. Effect of pitch on heat transfer characteristics of helical coils to be used for biogas production. Intl. J. Res. Eng. Technol., 4: 355-362.

Holman, J.P. and W.J. Gajda, 1989. Experimental Methods for Engineers. 5th Edn., McGraw-Hill Education, New York, USA., ISBN:9780070296220, Pages: 549.

Janssen, L.A.M. and C.J. Hoogendoorn, 1978. Laminar convective heat transfer in helical coiled tubes. Intl. J. Heat Mass Transfer, 21: 1197-1206.

Kozo, F. and A. Yoshiyuki, 1988. Laminar heat transfer in a helically coiled tube. Intl. J. Heat Mass Transfer, 31: 387-396.

Launder, B.E. and D.B. Spalding, 1972. Lectures in Mathematical Models of Turbulence. Academic Press, London, England.

Moawed, M., 2005. Experimental investigation of natural convection from vertical and horizontal helicoidal pipes in HVAC applications. Energy Convers. Manage., 46: 2996-3013.

Mohammed, H., 2011. Experimental study of free convection in coiled tube heat exchanger. Tikrit J. Eng. Sci., 18: 80-87.

Mohammed, H.A. and K. Narrein, 2012. Thermal and hydraulic characteristics of nanofluid flow in a helically coiled tube heat exchanger. Int. Commun. Heat Mass Transfer, 39: 1375-1383.

Pandey, A.K., P.K. Mishra and K.K. Srivastava, 2014. Experimental investigation of pressure drop inside a vertical helically coiled tube of curvature ratio 0.012. Intl. J. Eng. Sci. Res., 4: 398-401.

Pawar, S.S. and V.K. Sunnapwar, 2013. Experimental studies on heat transfer to Newtonian and non-Newtonian fluids in helical coils with laminar and turbulent flow. Exp. Therm. Fluid Sci., 44: 792-804.

Prabhanjan, D.G., T.J. Rennie and G.V. Raghavan, 2004. Natural convection heat transfer from helical coiled tubes. Intl. J. Therm. Sci., 43: 359-365.

Prahhanjan, D.G., 2000. Influence of coil characteristics on heat transfer to newtonians fluids. MSc Thesis, McGill University, Montreal, Canada.

Purandare, P.S., M.M. Lele and R. Gupta, 2012. Parametric analysis of helical coil heat exchanger. Intl. J. Eng. Res. Technol., 1: 1-5.

Rainieri, S., F. Bozzoli and G. Pagliarini, 2012. Experimental investigation on the convective heat transfer in straight and coiled corrugated tubes for highly viscous fluids: Preliminary results. Intl. J. Heat Mass Transfer, 55: 498-504.

Rogers, G.F.C. and Y.R. Mayhew, 1964. Heat transfer and pressure loss in helically coiled tubes with turbulent flow. Intl. J. Heat Mass Transfer, 7: 1207-1216.

Salimpour, M.R., 2009. Heat transfer coefficients of shell and coiled tube heat exchangers. Exp. Therm. Fuid Si., 33: 203-207.

Shokouhmand, H., M.R. Salimpour and M.A. Akhavan-Behabadi, 2008. Experimental investigation of shell and coiled tube heat exchangers using Wilson plots. Intl. Commun. Heat Mass Transfer, 35: 84-92.

Xin, R.C. and M.A. Ebadian, 1996. Natural convection heat transfer from helicoidal pipes. J. Thermophys. Heat Transfer, 10: 297-302.

Yang, G. and M.A. Ebadian, 1996. Turbulent forced convection in a helicoidal pipe with substantial pitch. Intl. J. Heat Mass Transfer, 39: 2015-2022.